HERA-19 Commissioning: A closer look at closure
HERA Memorandum Number 35
September 2017

C.L. Carilli[1,2], B. Nikolic[2]

ccarilli@aoc.nrao.edu

ABSTRACT

Using new CASA tools, we investigate closure phase behavior on redundant triads using HERA19 data. We consider data from HERA19 on the Bernardi source field at 21:00, and a high latitude field at 22:00. We find that the redundancy of the closure spectra improves with simpler fields (eg. two bright sources in main beam), and with longer baselines. This behavior is as expected if the non-redundancy is due to differences in the primary beam responses, coupled with the fact that the correlated signal can be dominated by diffuse emission filling the primary beams on these short spacings. Considering a strictly East-West oriented triad, the dispersion in the closure phase for redundant triads is between 6^o to 16^o over most of the spectra. These rms values translate into non-redundancy between baselines typically between 1.5% to 4%, as a function of frequency. We show that triads with a cross polarized antenna can still show coherence in the closure phase spectra, but the spectral behavior is completely different relative to normal triads, and would easily be seen in diagnostics based on redundant closure spectra. We investigate closure amplitudes. The closure amplitudes can diverge due to the division involved in the calculation.

1. Data and Processing

We investgate closure phase spectra for HERA19 data from June, 2016. This memo continues the work in HERA memos 13 and 15. The configuration and antenna numbers are given in Figure 1 in Memo 15. We employ the following two 10min data sets:

[1]National Radio Astronomy Observatory, P. O. Box 0, Socorro, NM 87801

[2]Cavendish laboratory, Cambridge University, UK

- zen.2457545.60538.xx.HH.uvcU = the field with two bright sources, as pointed out by G. Bernardi. The field center is 2056-3047 J2000 (see figure 1 in HERA memo 33). The two sources are: J2107-2519 with a flux density of 34Jy at 150MHz, and J2101-2802 with a flux density of 22Jy at 150MHz.

- zen.2457545.65410.xx.HH.uvcU.fits = a high latitude field with no obvious bright sources at 2206-3048.

We use the new task: CCLOSURE[1], incorporated into CASA in Socorro by B. Nikolic. This program generates .npz files with closure phase values as a function of frequency for specified triads of antennas. We have written python scripts to read, plot, and analyze the closure spectra.

We have investigated the closure phase spectra for both calibrated and uncalibrated data. The results are unchanged before and after calibration, as expected for closure quantities, when applying strictly antenna-based calibration solutions.

2. Results

2.1. Closure Phase Spectra

Figure 1 shows the closure phase spectra for the Bernardi source field for the different sets of redundant triads, starting from the smallest isosceles triads (15m baselines), to the next larger isosceles triads (30m baselines), and then using longer baselines (out to 45m). In the latter case, the triads are no longer isosceles due to array limitations. Visually, the redundancy appears to improve with increasing baseline length. In particular, for the shortest triad there are two frequency ranges (around 147MHz and 173MHz), when the sign of the closure phase reverse for different triads. Such reversals appear do not appear in the longer triads. We investigate these sign reversals further below.

Figure 2 shows the same type closure spectra for triads of increasing length, but now for the high latitude field with no dominant point sources. The behavior is qualitatively similar to the Bernardi source field with increasing triad length, except the signal to noise is lower, and there is more overall structure in the closure spectra, and a larger scatter between redundant triads.

---

[1]http://www.mrao.cam.ac.uk/ bn204/soft/py/heracasa/

Note that, if all our baselines were exactly redundant, then the curves for redundant triads in figures 1 and 2 should be coincident. Any non-coicidence indicates departures from redudancy.

The spectral behavior and depatures from redundancy seen in figures 1 and 2 can be understood in the context of non-redundancy caused by differences in the primary beam responses for different antennas, coupled with the fact that the correlated signal is dominated by diffuse emission filling the primary beams on short spacings. Primary beam differences can have multiple causes, including antenna position errors, feed focus, rotation and bore-site errors, dish surface errors, electromagnetic coupling between antennas, etc... The fact that the redundancy appears to get better with longer baselines, in particular for the Bernardi source field, is consistent with the correlated signal becoming dominated by two bright point sources within the FWHM of the primary beam. In this case beam errors are mitigated relative to the situation where the correlated signal is dominated by diffuse structures filling the full primary beam and sidelobes. A similar conclusion can be reached comparing the Bernardi source field and the high latitude field.

Figure 3 shows the closure phase spectra on strictly East-West triads, ie. triads made up of three consecutive antennas along an East-West row. These redundant triads show both cleaner behavior (no sign flips), and overall better redundancy, than the isosceles triads of Figure 1. This could be fortuitous, or may indicate something special about linear triads. Also shown in Figure 3 is the mean of the distribution of seven redundant E-W triads, and the rms of the distribution versus frequency. The lowest rms regions have dispesion values of $\sim 6^o$, while for most of the spectra, the rms ranges from 6^0 to 16^o, with a few ranges of higher dispersion. Using the logic outlined in memo 15, these rms values translate into non-redundancy between baselines typically between 1.5% to 4%, as a function of frequency.

Figure 4 shows two examples of the closure phase spectra for two of the shortest isosceles triads in the Bernardi source field (the orange and cyan curve from Figure 1). These two spectra demonstrate clearly the 'sign-flip' in the two spectral regions noted earlier (around 147MHz and 173MHz). To investigate this sign reversal, we also plot the calibrated visibility spectra for the baselines involved in each of the two triads. Note that the effective fringe frequency of a 15m baselines is about 8^o, and the source separation is 3.1^o. In each case, one of the baselines shows a large sweep in visibility phase in the two relevant narrow frequency ranges, although the sweep is of opposite sign in the two respective cases, leading to the sign flip in the closure spectra. Curiously, in each case this baseline has a fringe oriented roughly along the position angle separating the two sources, ie. these baselines have the least power to resolve the two sources. Our guess is that there must be some other large scale structure which is affecting these visibilities in this curious manner. As to origin of the sign reversal,

that remains unknown.

We next constructed a simple source model of two point sources with similar orientation, separation, and brightness ratio, as the two Bernardi sources. We then used the H37 configuration and the CASA simulator to generate a mock observation of the field. Figure 5 shows the results, including both the closure phase spectra on the shortest isosceles triad, and the next longest triad, and the visibility phase spectra for the antennas involved. The closure spectra for the shortest triad does not show any large sweep over a narrow frequency range for this simple model, supporting the conclusion above concerning larger scale structure affecting the observed visibilities. The longer triad does show large frequency sweeps, as expected since some baseline orientations will substantially resolve the source separation (fringe spacing now $\sim 4^o$).

We consider the question of how a cross polarized antenna appears in a closure analysis. Figure 6 shows closure phase spectra for the smallest isosceles triads and for the East-West oriented triads. The magenta curve in each case includes a known cross polarized antennas (antenna 81, I believe in AIPY numbering scheme). The other triads are normal, as per figures 1 and 3. The cross polarized spectra still show coherent structure in frequency, implying that there remains enough signal coming through the system to generate closure phase coherence, although the scatter in the cross polarized closure spectra is visibly larger than for the good triads. More importantly, the spectral structure for the triad including the cross polarized antenna is completely different than for the good triads. This difference would be seen clearly in any closure diagnostic analysis. On the other hand, the raw visibility amplitudes for the cross polarized antenna will be factors of many lower than normal visibilities, and should be obvious to any flagging scheme.

2.2. Closure Amplitude Spectra

For completeness, we calculate closure amplitudes. Closure amplitudes (CA), involve the product of four visibilities amplitudes (A):

$CA_{i,j,k,l} = [A_{ij}A_{kl}]/[A_{ik}A_{jl}]$

As with closure phase, the antenna based calibration terms in this product of visibilities cancel, and one is left with a 'true sky measurement', even for uncalibrated visibilities (see equation 10.44 in Thomson, Moran, Swenson 2017). A closure amplitude tool does not yet exist in CASA, so we employ the python script-based approach for calculation, as per HERA memo 15. We also use the same Galactic Center data from Memo 15.

Figure 7 shows the closure amplitudes for two short, redundant quadrangles: 54,105,65,81 and 90,66,21,32 (numbers as per memo 15). There is broad similarity, but there are large peaks in the distributions that do not replicate well between quadrangles. The reason is clear: the closure amplitude involves a division. Hence, if one of the visibility amplitudes goes through a null, or close to zero, any noise will blow-up the resulting closure amplitude.

The visibility amplitude spectra for the baselines in one of these quadrangles is shown in Figure 7 as well. Indeed, the peaks in the closure amplitude spectra occur when one or more of the visibility spectra approach zero.

3. Conclusions

- We find that the redundancy of the closure spectra improves with simpler fields (eg. two bright sources in the main beam), and with longer baselines. This behavior is as expected if the non-redundancy is due to differences in the primary beam responses (caused by antenna position errors, feed focus, rotation, and bore site errors, dish surface errors, etc...), coupled to the fact that the correlated signal can be dominated by diffuse emission filling the primary beam and sidelobes on these short spacings.

- The dispersion in the closure phase spectra for redundant triads for strictly East-West oriented triads ranges between 6^0 to 16^o over most of the spectra. These rms values translate into non-redundancy between baselines typically between 1.5% to 4%, as a function of frequency.

- We investigate the sign reversals in some narrow frequency ranges in redundant triad closure phase spectra. The results are inconclusive.

- Triads including a cross polarized antenna can still show coherence in the closure phase spectra, but the spectral behavior is completely different relative to normal triads, and would be obvious in any diagnostic based on closure phase spectra.

- We investigate closure amplitudes. While the behavior for redundant quadrangles are similar, the calculation of closure amplitude involves division, and the values can blow-up in regions when one or more of the visibility spectra approaches zero.

References

Carilli, C. 2016, HERA memo 15
(http://reionization.org/science/memos/)

Carilli, C., & Sims, P. 2016, HERA memo 12

Carilli, C., Nikolic, B., & Gale-Sides, K. 2016, HERA memo 23

Nikolic, B., Carilli, C., & Sims, P. 2016, HERA memo 22

Carilli, C., Nikolic, B., Gale-Sides, K., Bernardi, G. 2016, HERA memo 33

Thompson, A.R., Moran, J., Swenson, G. 2017, Interferometry and Synthesis in Radio Astronomy, John Wiley & Sons

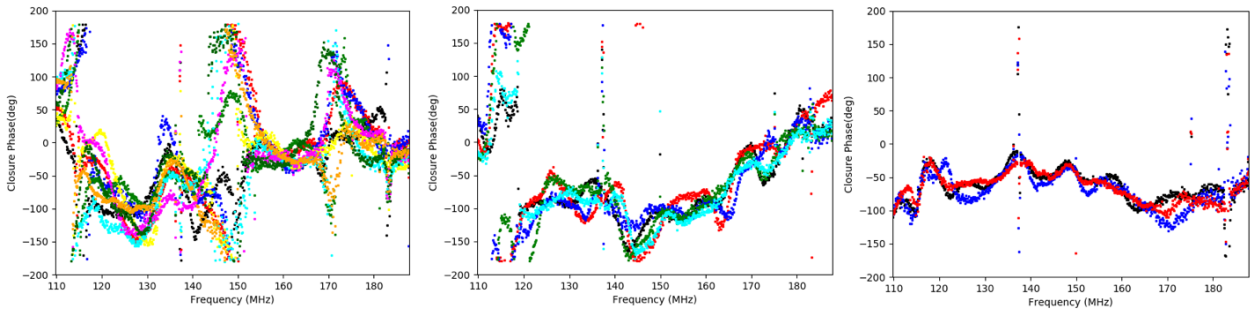

Fig. 1.— Left: Closure phase spectra on the shortest isosceles triad (15m baselines) for the Bernardi source field. Center: Same, but for the next longer isosceles triads (30m). Right: Same, but for a few even longer triads, including baselines of 45m length, although the triad is no longer isosceles.

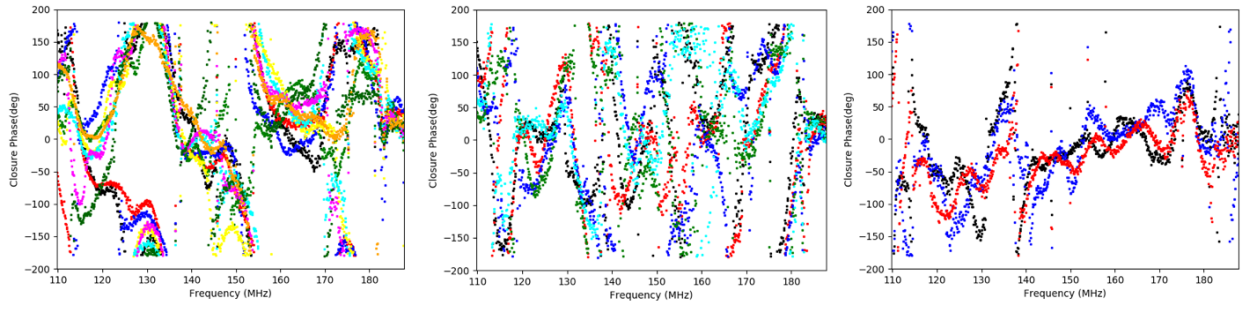

Fig. 2.— Left: Closure phase spectra on the shortest isosceles triad (15m baselines) for a high latitude field at RA = 22:00. Center: Same, but for the next longer isosceles triads (30m). Right: Same, but for a few even longer triads, including baselines of 45m length, although the triad is no longer isosceles.

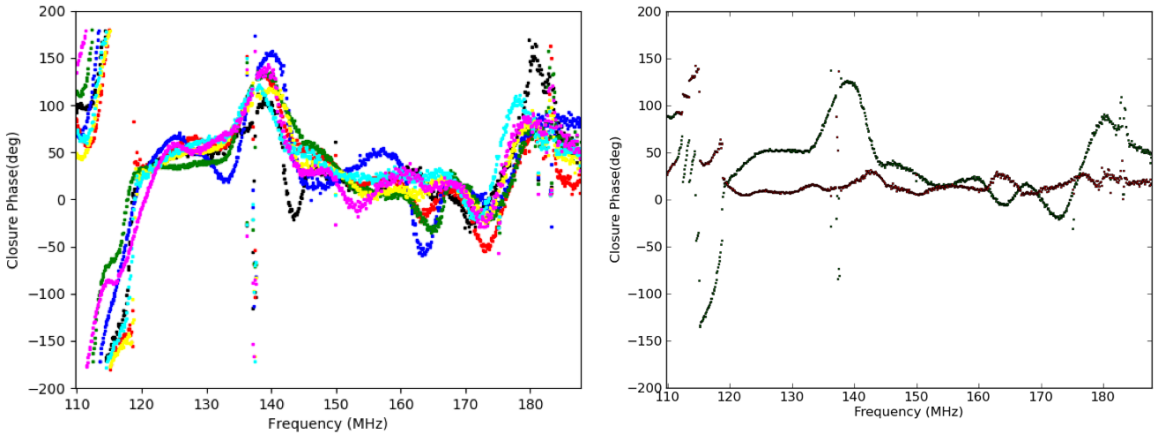

Fig. 3.— Left: Closure phase spectra on a strictly East-West triad of three consecutive antennas along a row, for the Bernardi source field. Right: Mean of the closure phases for the seven triads (green) plus the rms of the distribution (red).

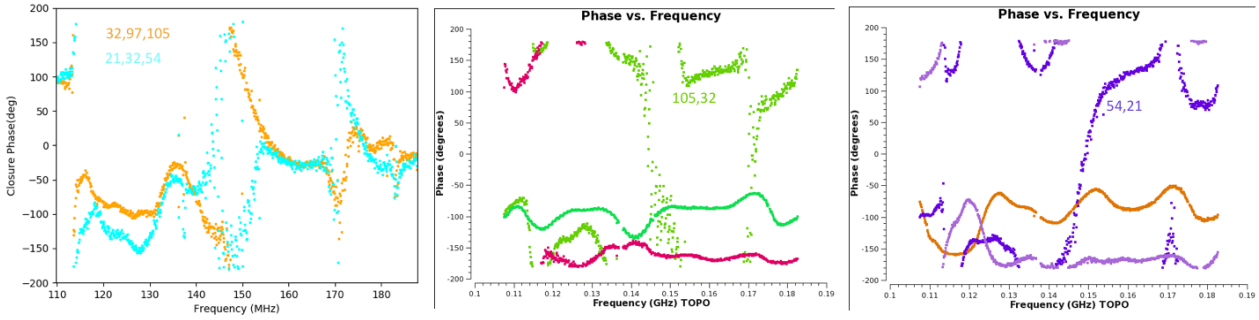

Fig. 4.— Left: Closure phase spectra on two of the shortest isosceles triad (15m baselines) for the Bernardi source field. These show the 'flip' in sign at around 147MHz and 173MHz. Center: Calibrated visibility spectra for the baselines involved in the orange curve in the figure on the left (32,97,105). Right: Calibrated visibility spectra for the baselines involved in the cyan curve in the figure on the left (21,32,54).

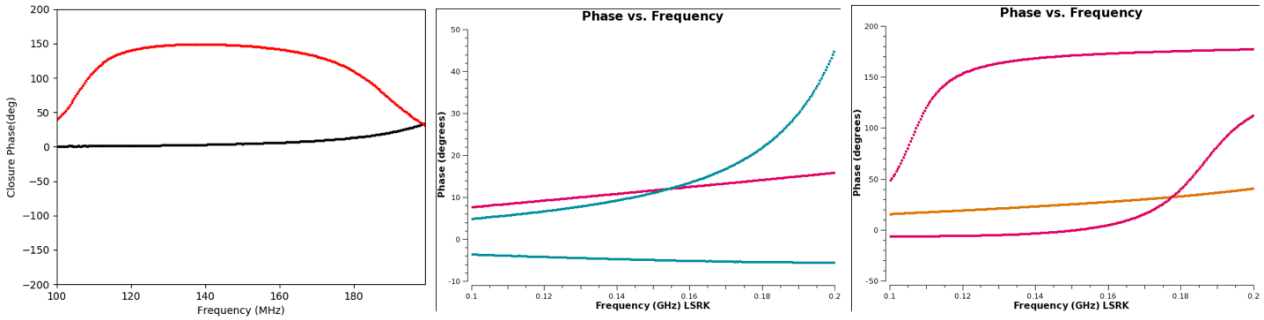

Fig. 5.— Left: Simulated closure phase spectra on isosceles triads of HERA, for a two point source model with a separation, orientation, and relative brightness comparable to the Bernardi sources (although the position in the beam was not exactly the same as the observed field, so there could be an overall shift in frequency). The black curve is for the shortest triad (15m), and the red is for the next longest (30m). Center: Visibility phase spectra for the shortest baselines (15m) involved in the black triad shown in the left hand frame. Right: Center: Visibility phase spectra for the next longest baselines (30m) involved in the red triad shown in the left hand frame.

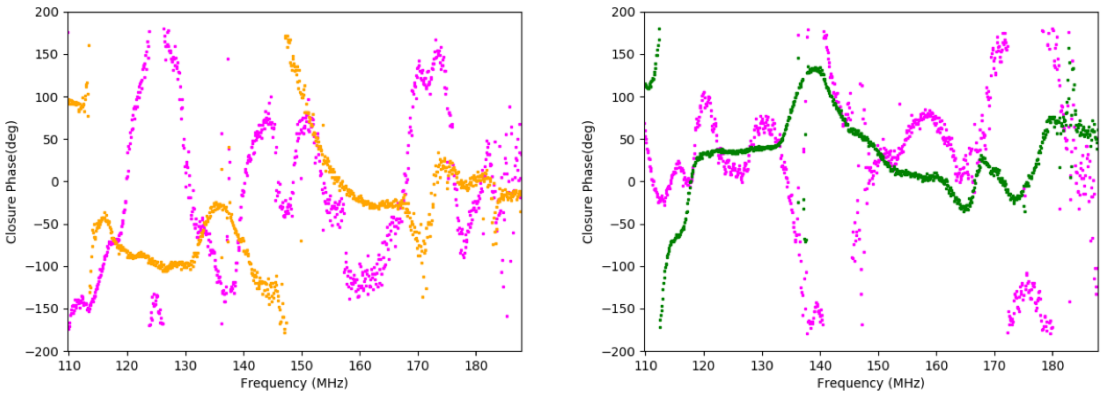

Fig. 6.— Left: closure phase spectra for the Bernardi field on the shortest isosceles triad. The orange curve is a typical spectrum for a normal triad, as per figure 1. The magenta curve includes a cross polarized antenna (81 in AIPY). Note that there remains enough signal to generate a coherent closure spectrum for the cross polarized antenna, but the spectrum itself bares no resemblance to the normal triad (see Figure 1). Right: Same, but for an East-West triad, as per Figure 3. Again, magenta is cross-polarized.

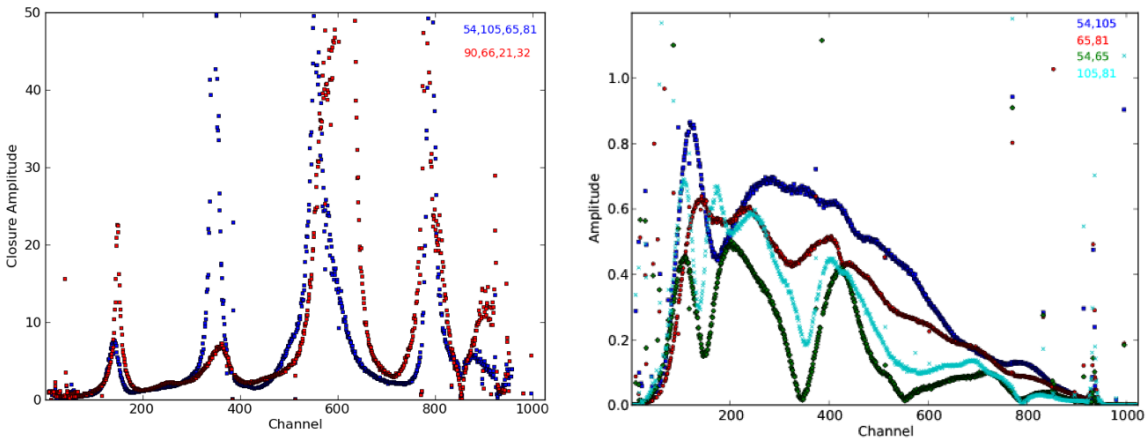

Fig. 7.— Left: closure amplitude spectra for the Galactic Center field for two short quadrangles. Right: the visibility amplitude spectra for the baselines involved in one of the quadrangles in the left plot.